



APCTP – BLTP JINR

7th International Workshop

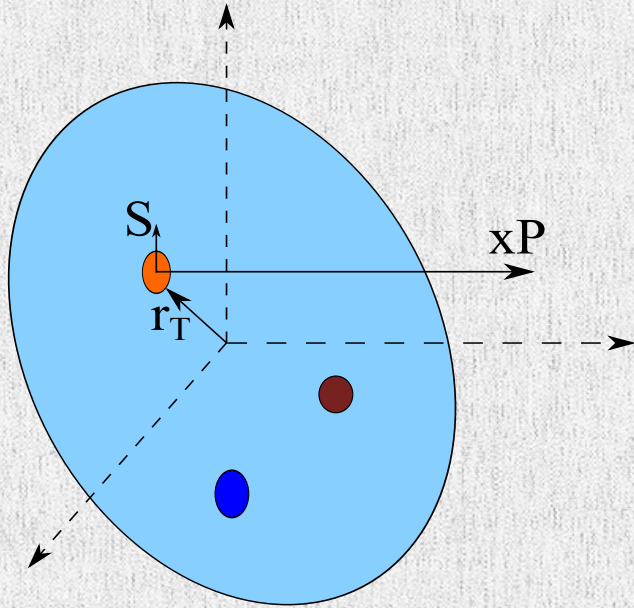
July 14-19, 2013, Baikal



DEEPLY VIRTUAL EXCLUSIVE PRODUCTION ON LONGITUDINALLY POLARIZED PROTON WITH CLAS

Andrey Kim and Wooyoung Kim
Kyungpook National University

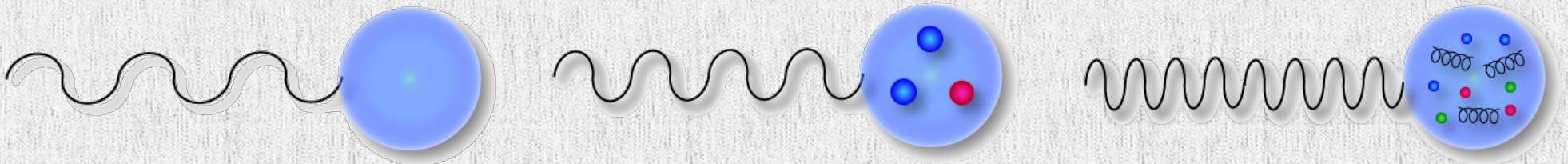
INTRODUCTION



Deeply virtual exclusive reactions such as photon or π^0 meson production with large gamma virtuality Q^2 are key processes to probe the complex internal structure of nucleon and access information about quark position and angular momentum distributions from experimental observables.

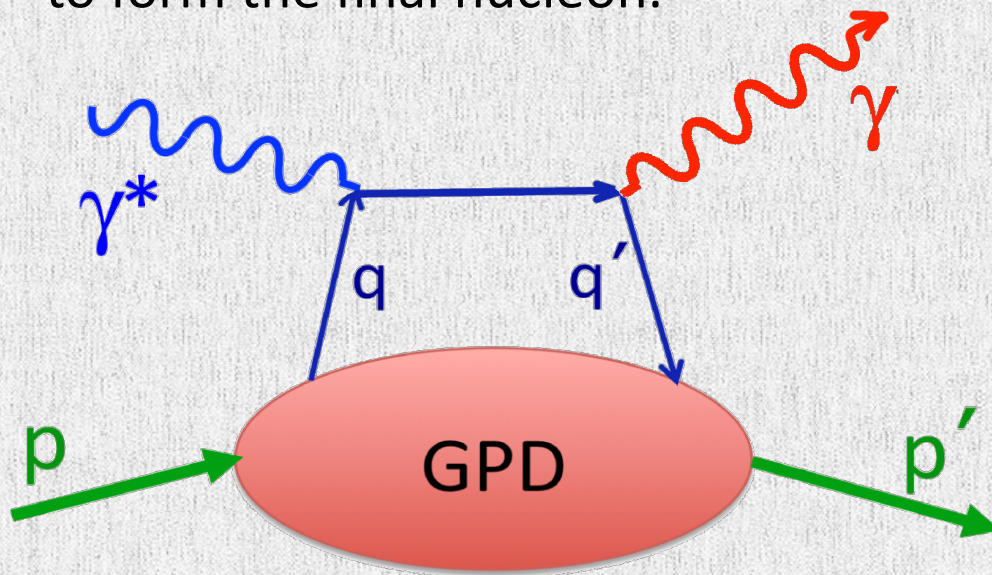
Two main processes can be used to access this information experimentally:

Deeply Virtual Compton Scattering and **Deeply Virtual Meson Production**



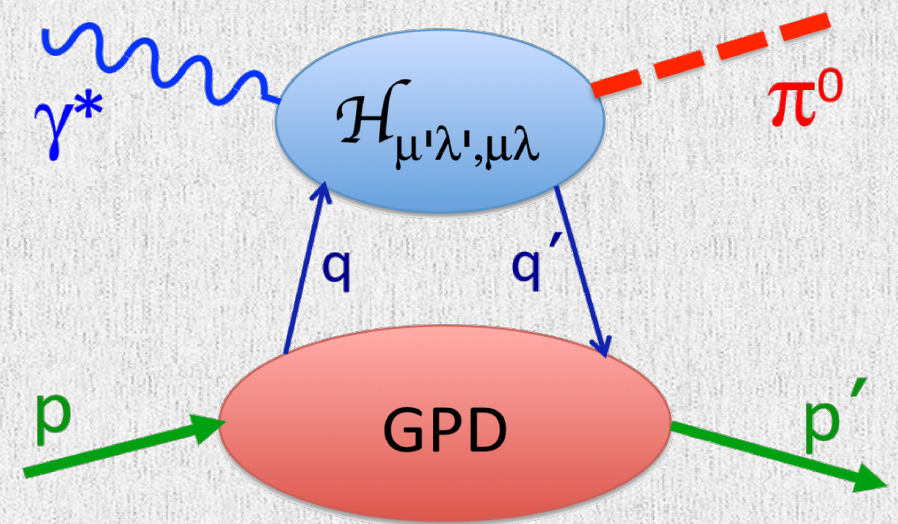
DEEPLY VIRTUAL EXCLUSIVE REACTIONS

Subprocess of virtual photon interacting with a single quark with momentum fraction x in the nucleon to produce a meson and returning quark, which is absorbed to form the final nucleon.



Deeply Virtual Compton Scattering in the framework of the handbag mechanism

π^0 electroproduction amplitude in the framework of the handbag mechanism



GPD encodes the distribution of the quark and gluon momentum fractions and transverse spatial distributions within the nucleon.

GENERALIZED PARTON DISTRIBUTIONS

H^q	\tilde{H}^q	E^q	\tilde{E}^q	parton helicity conserving (chiral-even) GPDs
H_T^q	\tilde{H}_T^q	E_T^q	\tilde{E}_T^q	parton helicity-flip (chiral-odd) GPDs

For π^0 electroproduction the GPDs appear in the flavor combinations:

$$F_i^{\pi^0} = (e_u F_i^u - e_d F_i^d) / \sqrt{2}$$

x	average parton momentum fraction
$\xi \simeq \frac{2x_B}{2-x_B}$	(skewness) difference between the initial and final fractions of the longitudinal momentum carried by the struck parton
$t = (p - p')^2$	momentum transfer between initial and final nucleons

The GPDs depend on three kinematic variables,

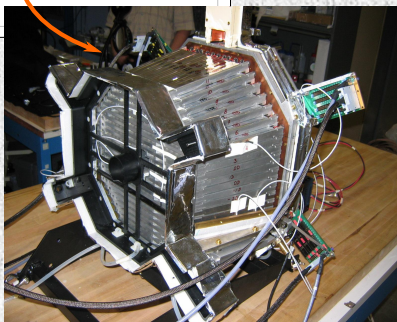
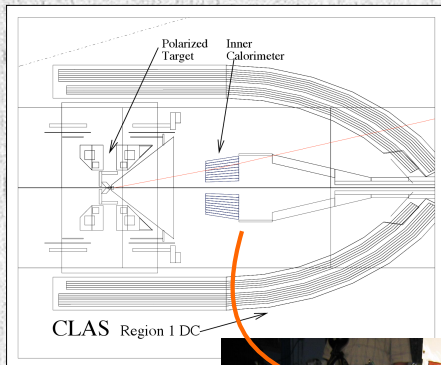
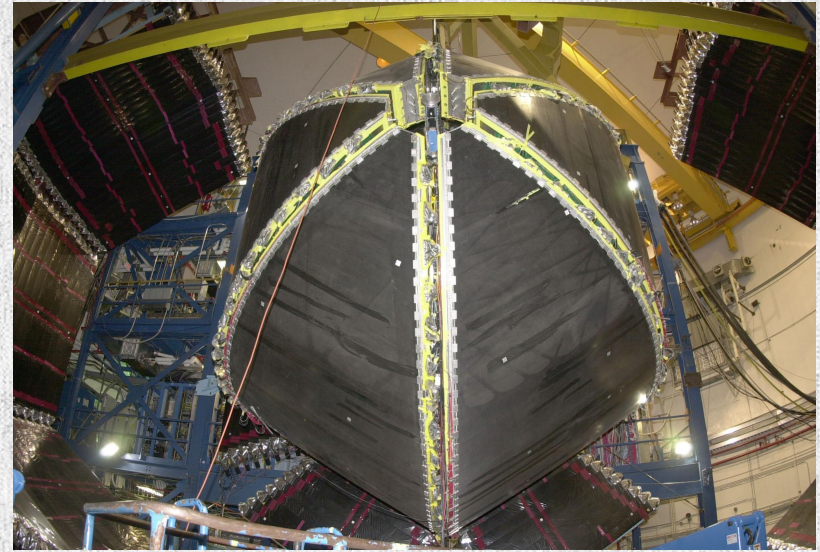
e.g. $H^q(x, \xi, t)$

EXPERIMENTAL SETUP

The presented experimental data were taken at Jefferson Lab:

- The data were collected between February and September 2009
- CEBAF provided a longitudinally polarized electron beam (>80%)
- CEBAF Large Acceptance Spectrometer was used to detect outgoing particles
- The incident electron beam energy was approximately 6 GeV
- The integrated luminosity was 75 fb^{-1}
- The target was longitudinally polarized $^{14}\text{NH}_3$

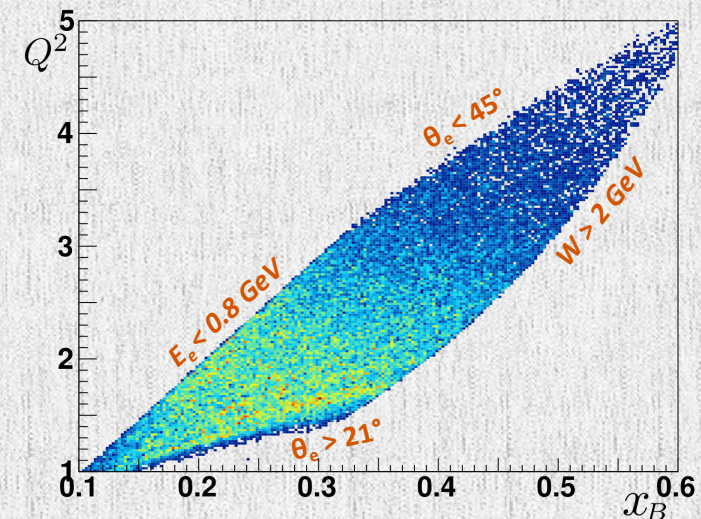
Inner Calorimeter was used to detect high energy photons at small angles



The Inner Calorimeter (IC):

1. is an additional calorimeter inserted to the standard CLAS configuration downstream of the target.
2. detects photons from decay of the neutral pions in the forward direction and **increase the detection of photons in the range from 5° up to 16° .**
3. blocks charged particles permitting detection of the **protons in angular range 18° to 50° , and electrons - from 18° to 45° .**

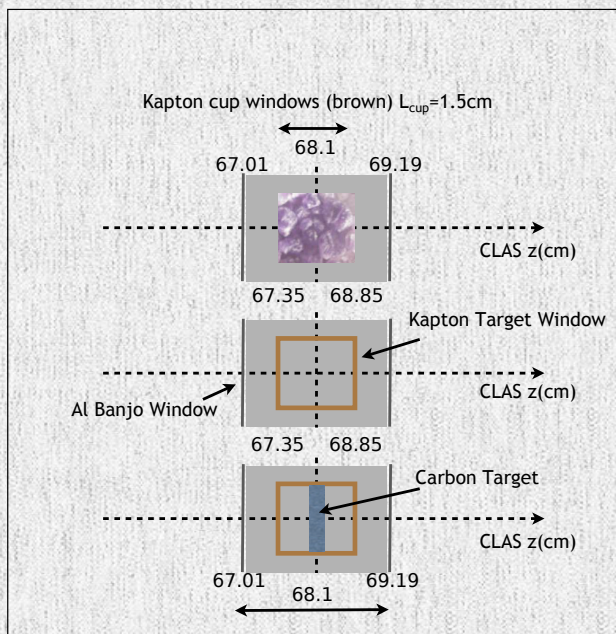
ELECTRON KINEMATICS



LONGITUDINALLY POLARIZED TARGET

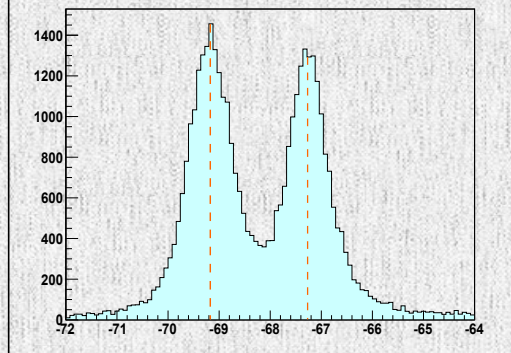
- ◆ Frozen ammonia was used as a target
- ◆ It was longitudinally polarized using Dynamic Nuclear Polarization (DNP)
- ◆ The polarization was monitored using a Nuclear Magnetic Resonance (NMR) system

The side view of the target material in CLAS. Ammonia, empty and carbon (top to bottom) targets are shown here with a central nominal vertex.

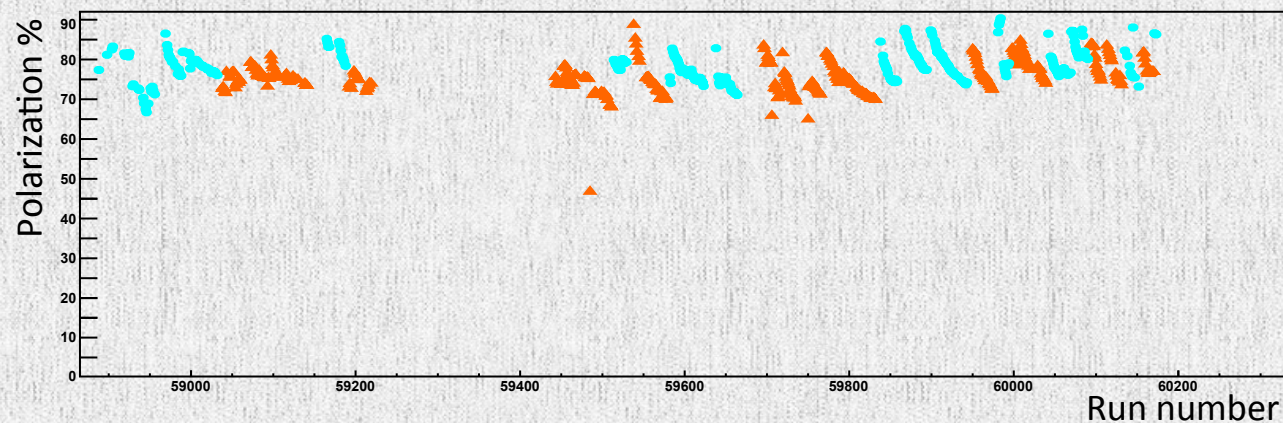


Al Banjo Windows $L \sim 2.18$ cm
Liquid ^4He filled (light gray shading)

Reconstructed electron vertex for run with empty target. Two peaks corresponds to the aluminum banjo windows



NRM target polarization during eg1dvcs experiment

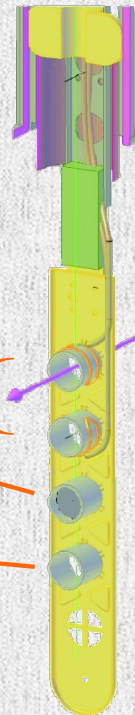


· Crushed beads of irradiated ammonia prepared at University of Virginia

· Disk of amorphous carbon

· Empty

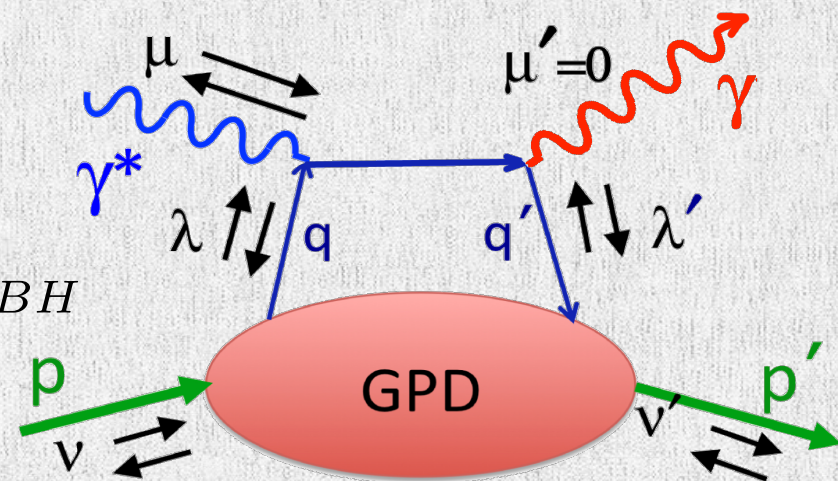
The last two cells are utilized for background studies.



ACCESSING GPDs THROUGH DVCS

$$\frac{d\sigma}{dx_B dQ^2 dt d\phi} \sim |T|^2 = |T_{BH} + T_{DVCS}|^2$$

$$= |T_{BH}|^2 + |T_{DVCS}|^2 + T_{DVCS} T_{BH}^* + T_{DVCS}^* T_{BH}$$



$$A_{LU} \sim \text{Im} \left\{ F_1 H + \xi (F_1 + F_2) \tilde{H} + \frac{t}{4M^2} F_2 E \right\} \sin \phi$$

Kinematically suppressed in CLAS kinematics

$$A_{UL} \sim \text{Im} \left\{ F_1 \tilde{H} + \xi (F_1 + F_2) \left(H - \frac{x_B}{2} E \right) - \xi \left(\frac{x_B}{2} F_1 - \frac{t}{4M^2} F_2 \right) \tilde{E} \right\} \sin \phi$$

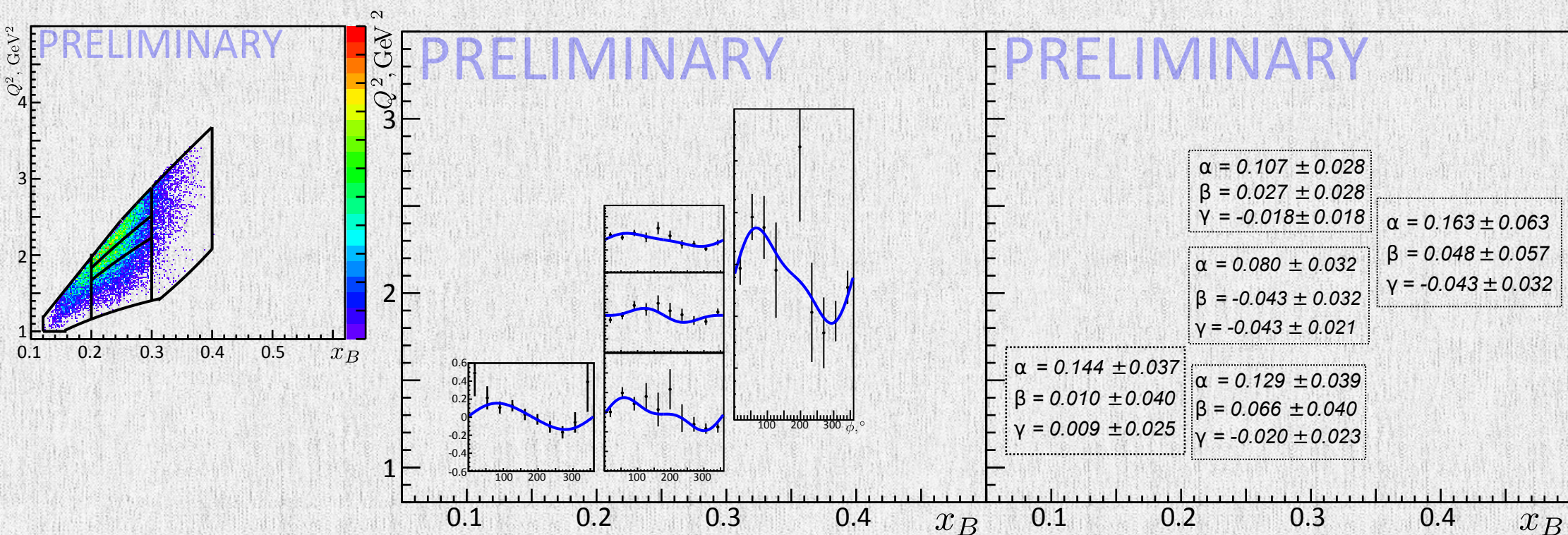
DVCS TARGET SPIN ASYMMETRIES

- ◆ The target spin asymmetries were fitted: $A_{UL} = \alpha \sin \phi + \beta \sin 2\phi + \gamma$
- ◆ Future plans:
 - ▣ π^0 background subtraction
 - ▣ Double spin asymmetries measurements

$0.08 < -t < 0.2 \text{ GeV}^2$

$0.2 < -t < 0.5 \text{ GeV}^2$

$0.5 < -t < 1.8 \text{ GeV}^2$



The plots provided by E. Seder

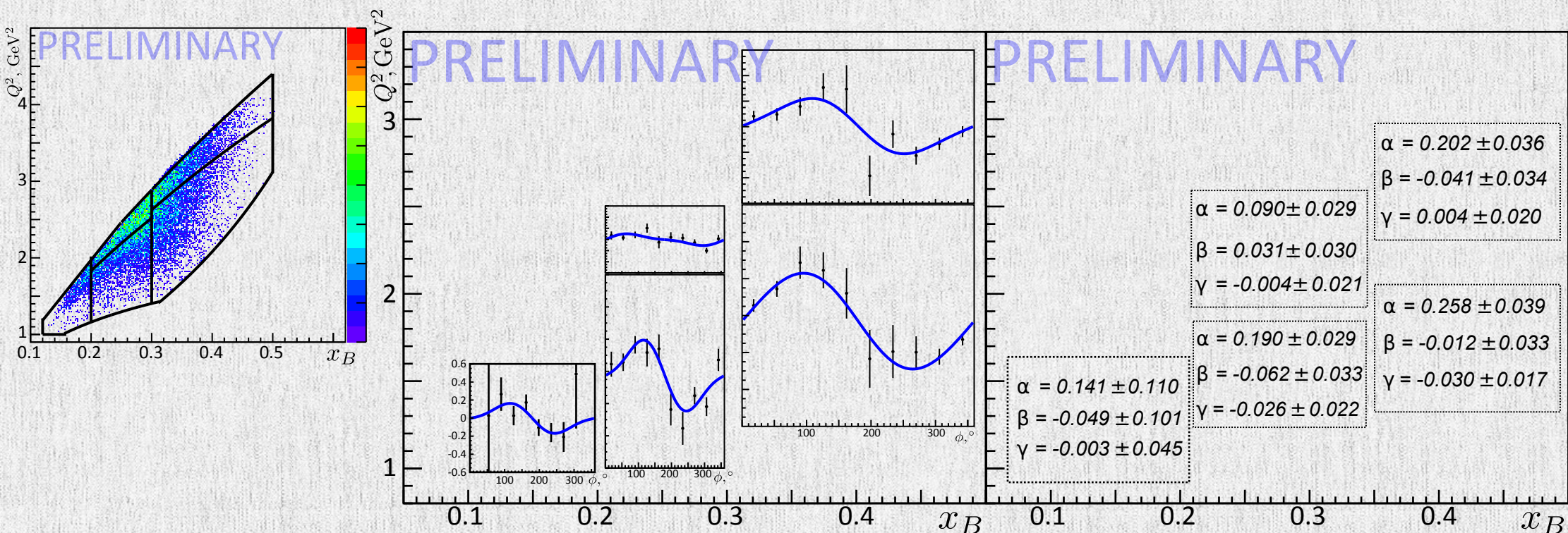
DVCS TARGET SPIN ASYMMETRIES

- ◆ The target spin asymmetries were fitted: $A_{UL} = \alpha \sin \phi + \beta \sin 2\phi + \gamma$
- ◆ Future plans:
 - ▣ π^0 background subtraction
 - ▣ Double spin asymmetries measurements

$0.08 < -t < 0.2 \text{ GeV}^2$

$0.2 < -t < 0.5 \text{ GeV}^2$

$0.5 < -t < 1.8 \text{ GeV}^2$



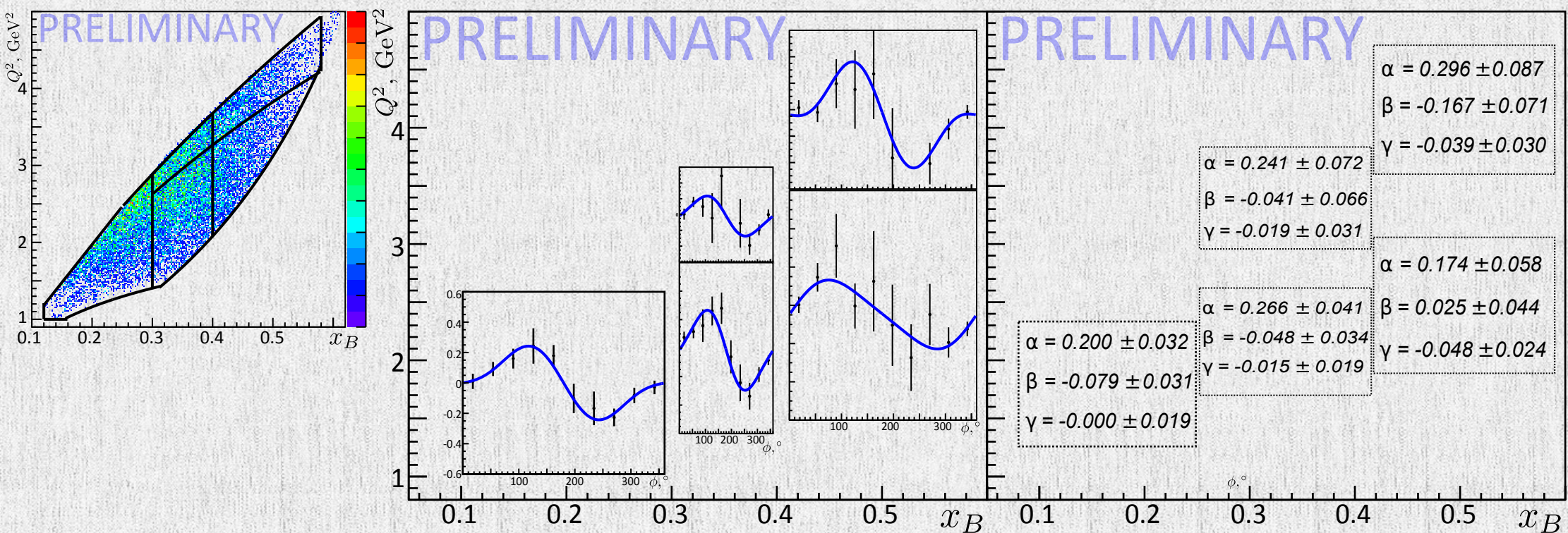
DVCS TARGET SPIN ASYMMETRIES

- ◆ The target spin asymmetries were fitted: $A_{UL} = \alpha \sin \phi + \beta \sin 2\phi + \gamma$
- ◆ Future plans:
 - ▣ π^0 background subtraction
 - ▣ Double spin asymmetries measurements

$0.08 < -t < 0.2 \text{ GeV}^2$

$0.2 < -t < 0.5 \text{ GeV}^2$

$0.5 < -t < 1.8 \text{ GeV}^2$



DV π^0 P STRUCTURE FUNCTIONS

$$\frac{2\pi}{\Gamma} \frac{d^4\sigma}{dQ^2 dx_B dt d\phi_\pi} =$$

$$\sigma_T + \epsilon\sigma_L + \epsilon\sigma_{TT} \cos 2\phi + \sqrt{\epsilon(1+\epsilon)}\sigma_{LT} \cos \phi$$

unpolarized terms

longitudinally
polarized target

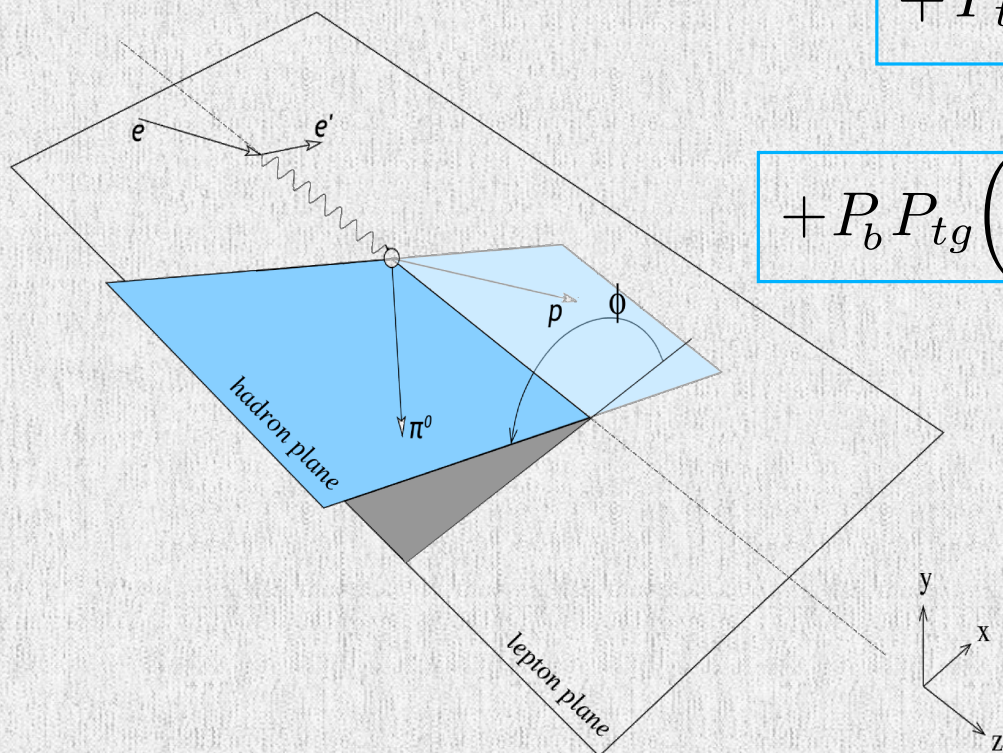
longitudinally
polarized beam

$$+ P_b \sqrt{\epsilon(1-\epsilon)}\sigma_{LT'} \sin \phi$$

$$+ P_{tg} \left(\sqrt{\epsilon(1+\epsilon)}\sigma_{UL}^{\sin \phi} \sin \phi + \epsilon\sigma_{UL}^{\sin 2\phi} \sin 2\phi \right)$$

$$+ P_b P_{tg} \left(\sqrt{1-\epsilon^2}\sigma_{LL} + \sqrt{\epsilon(1-\epsilon)}\sigma_{LL}^{\cos \phi} \cos \phi \right)$$

longitudinally polarized beam
and
longitudinally polarized target



ACCESSING GPDs THROUGH DV π^0 P

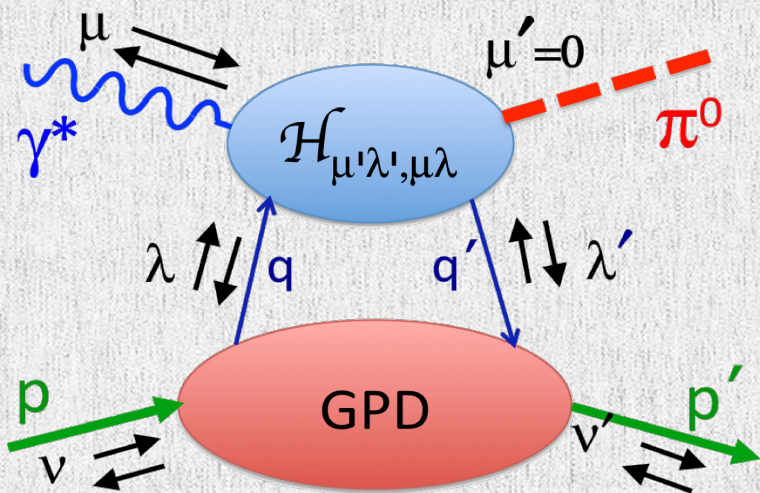
UNPOLARIZED STRUCTURE FUNCTIONS:

$$\sigma_L \sim \left\{ (1 - \xi^2) |\langle \tilde{H} \rangle|^2 - 2\xi^2 \text{Re} [\langle \tilde{H} \rangle^* \langle \tilde{E} \rangle] - \frac{t'}{4m^2} \xi^2 |\langle \tilde{E} \rangle|^2 \right\}$$

$$\sigma_T \sim \left[(1 - \xi^2) |\langle H_T \rangle|^2 - \frac{t'}{8m^2} |\langle E_T \rangle|^2 \right]$$

$$\sigma_{TT} \sim |\langle \bar{E}_T \rangle|^2$$

POLARIZED OBSERVABLES:



$$A_{LU}^{\sin \phi} \sigma_0 \sim \text{Im} [\langle H_T \rangle^* \langle \tilde{E} \rangle]$$

$$A_{UL}^{\sin \phi} \sigma_0 \sim \text{Im} [\langle \bar{E}_T \rangle^* \langle \tilde{H} \rangle + \xi \langle H_T \rangle^* \langle \tilde{E} \rangle]$$

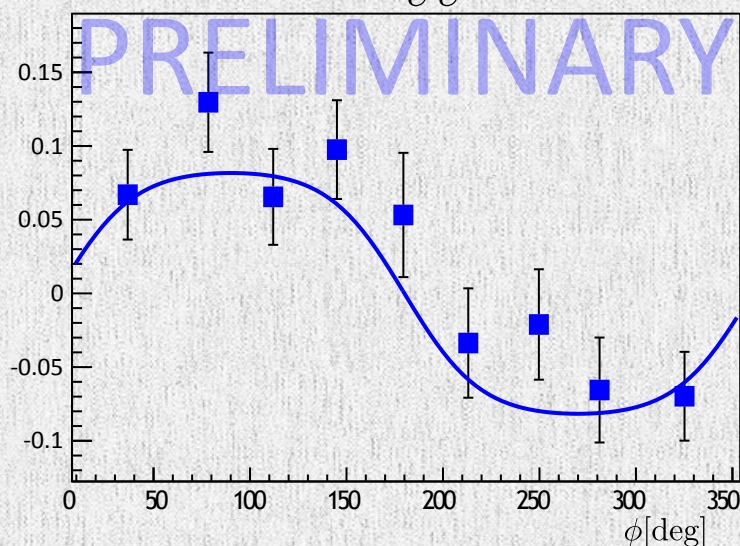
$$A_{LL}^{\cos 0\phi} \sigma_0 \sim |\langle H_T \rangle|^2$$

$$A_{LL}^{\cos \phi} \sigma_0 \sim \text{Re} [\langle \bar{E}_T \rangle^* \langle \tilde{H} \rangle + \xi \langle H_T \rangle^* \langle \tilde{E} \rangle]$$

DV π^0 P SPIN ASYMMETRIES

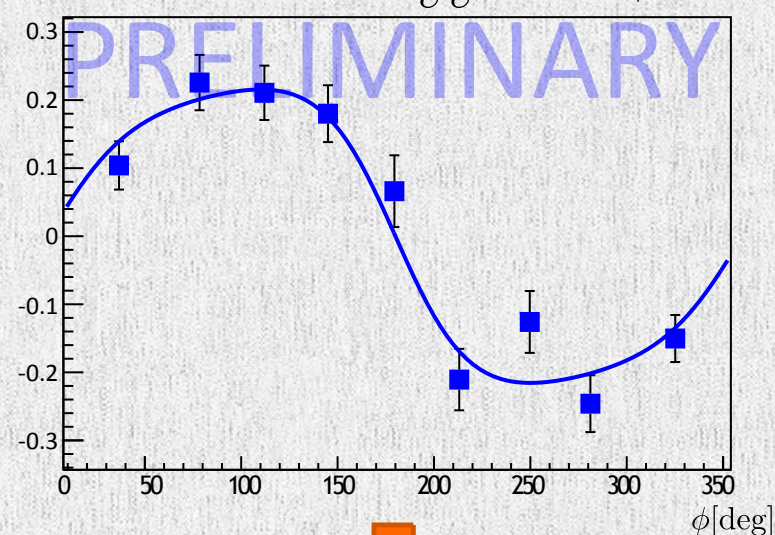
BEAM SPIN ASYMMETRY

$$A_{LU} = \frac{A_{LU}^{\sin \phi} \sin \phi}{1 + A_{UU}^{\cos 2\phi} \cos 2\phi}$$



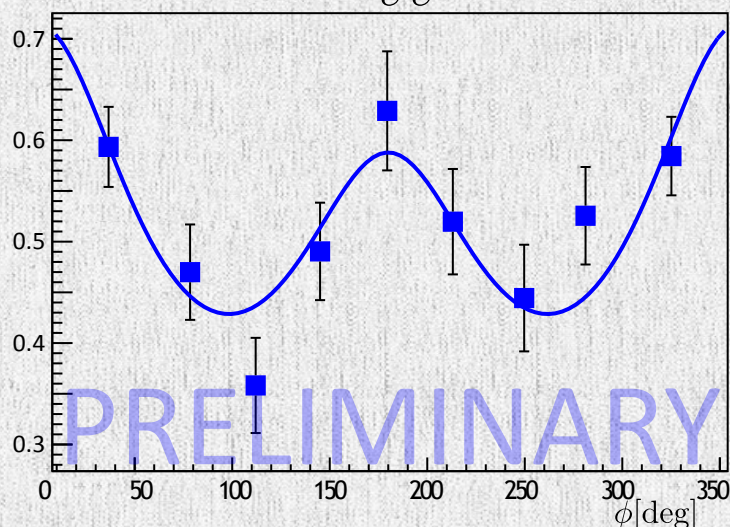
TARGET SPIN ASYMMETRY

$$A_{UL} = \frac{A_{UL}^{\sin \phi} \sin \phi + A_{UL}^{\sin 2\phi} \sin 2\phi}{1 + A_{UU}^{\cos 2\phi} \cos 2\phi}$$



DOUBLE SPIN ASYMMETRY

$$A_{LL} = \frac{A_{LL}^{const} + A_{LL}^{\cos \phi} \cos \phi}{1 + A_{UU}^{\cos 2\phi} \cos 2\phi}$$



The data were **fitted simultaneously** with 6 parameters:

1. $A_{UU}^{\cos 2\phi}$
2. $A_{LU}^{\sin \phi}$
3. $A_{UL}^{\sin \phi}$
4. $A_{UL}^{\sin 2\phi}$
5. A_{LL}^{const}
6. $A_{LL}^{\cos \phi}$

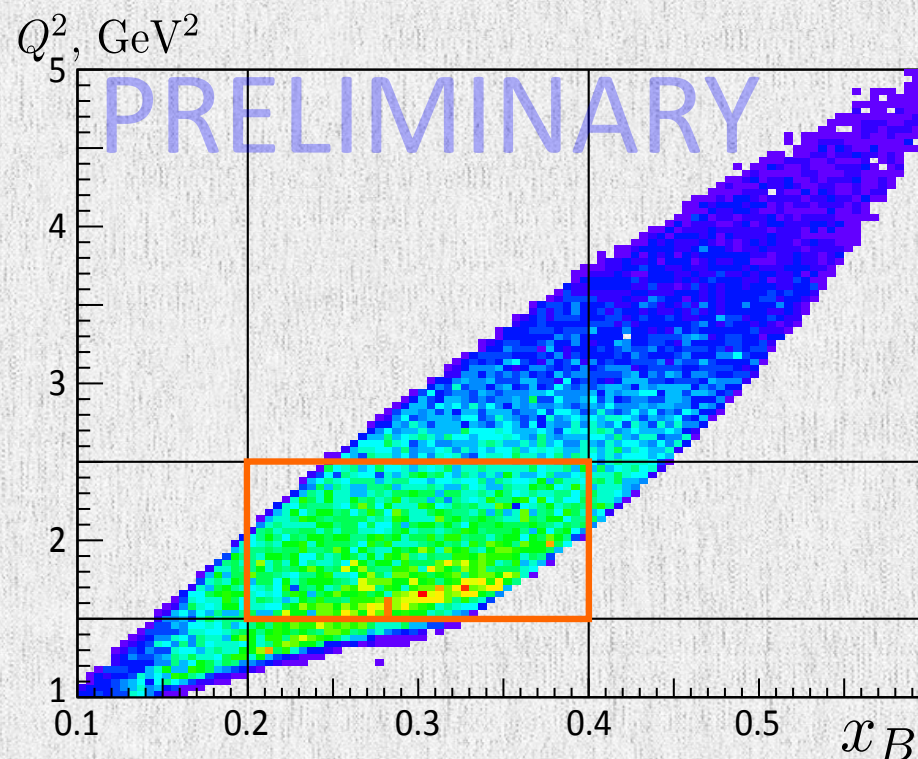
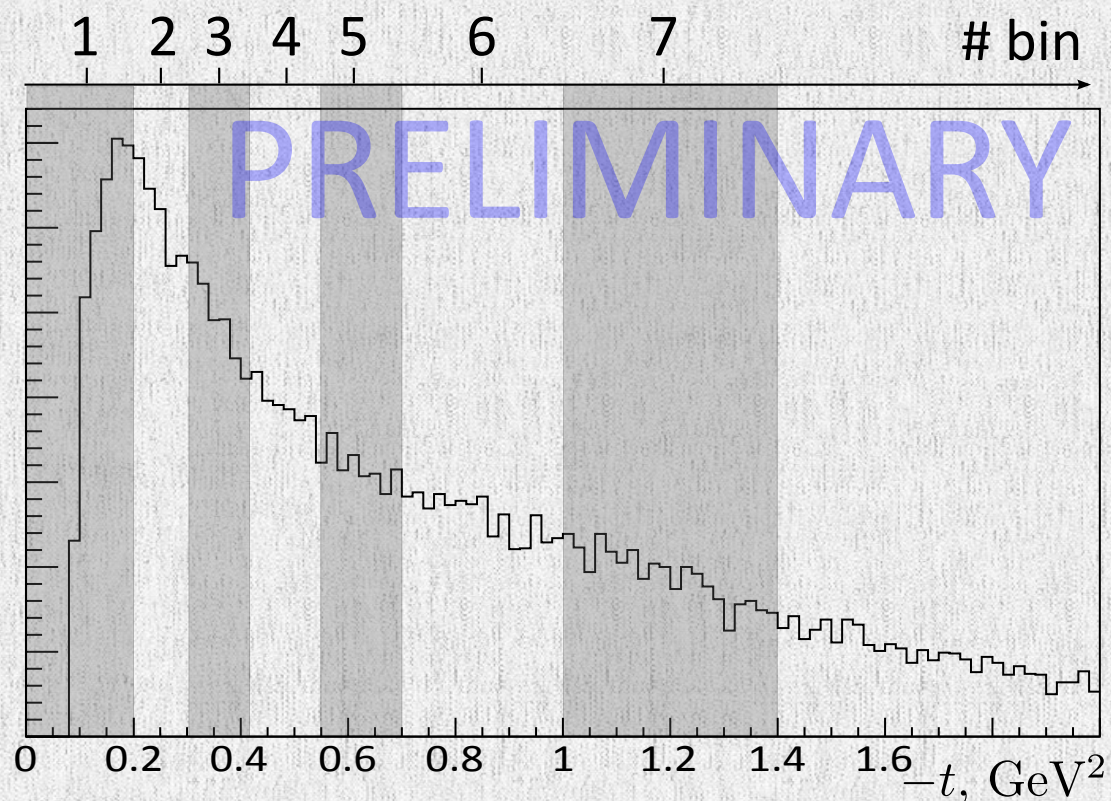
The data were integrated over wide range of Q^2 , x_B and t'

DV π^0 P BINNING

- ◆ 1 bin in Q^2
- ◆ 1 bin in x_B
- ◆ 7 bins in t
- ◆ 9 bins in ϕ

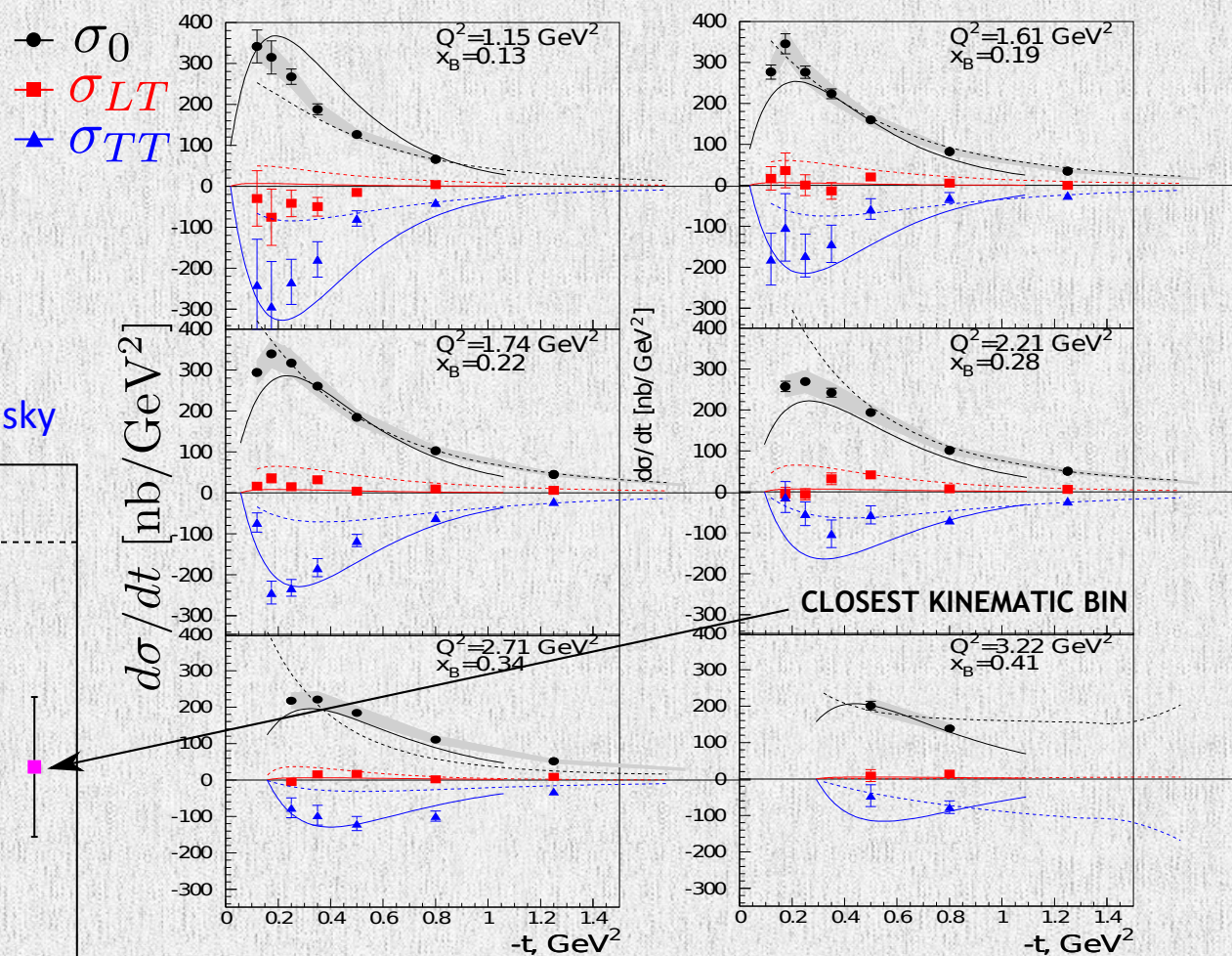
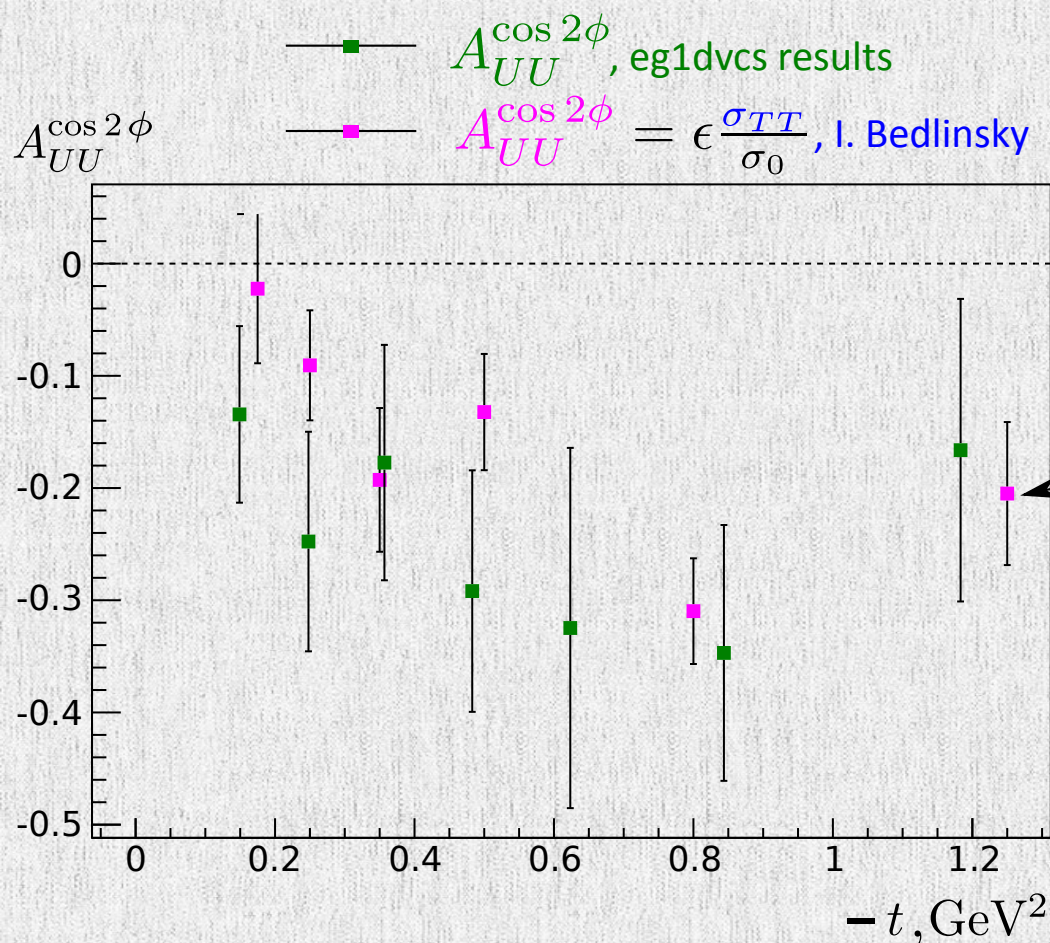
$$1.5 < Q^2 < 2.5 \text{ GeV}^2$$

$$0.2 < x_B < 0.4$$



DV π^0 P UNPOLARIZED TERMS

The results of fit for unpolarized parameter agree with previous CLAS results, considering the difference in kinematic coverage.

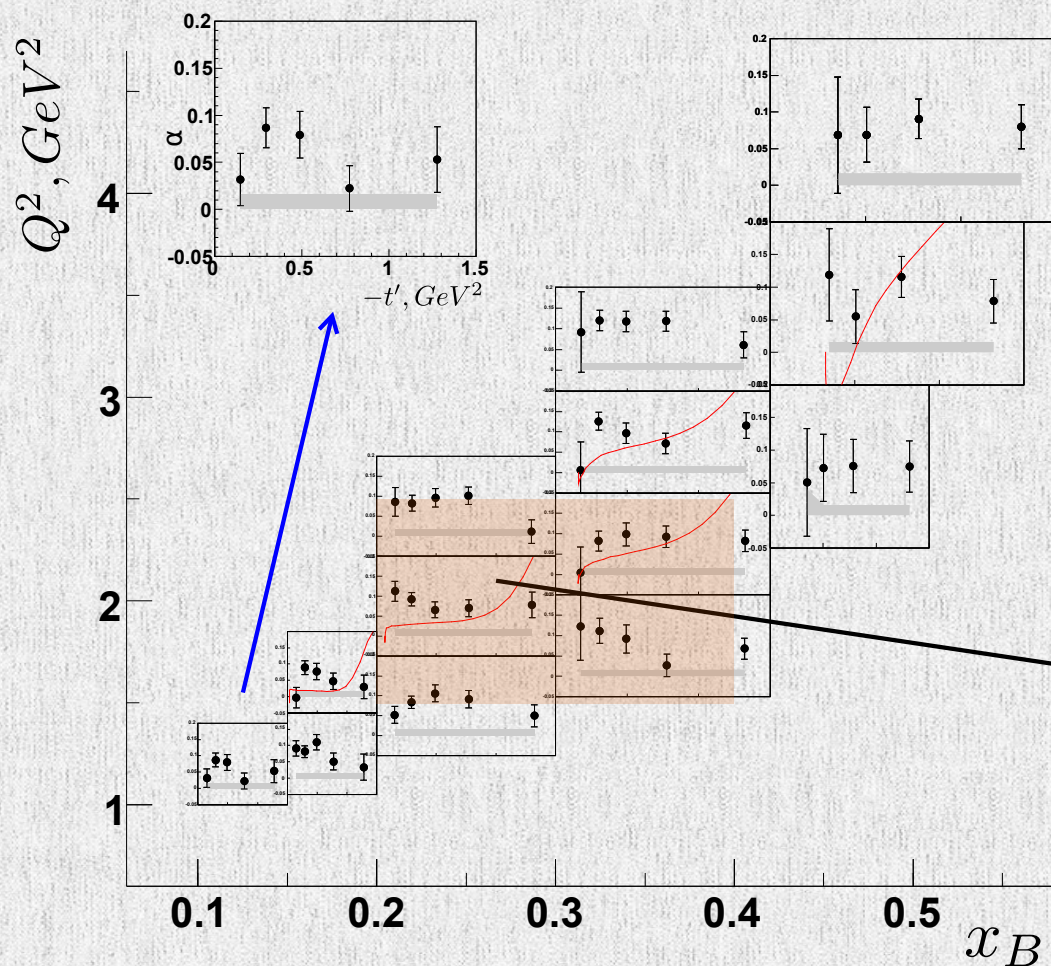


I. Bedlinskiy *et al.* Measurement of Exclusive π^0 Electroproduction Structure Functions and their Relationship to Transversity GPDs. 2012.

solid curve: P.Kroll & S.Goloskokov arXiv:1106.4897

dashed curve: G.R. Goldstein, J.O. Gonzalez & S.Liuti arXiv:1012.3776

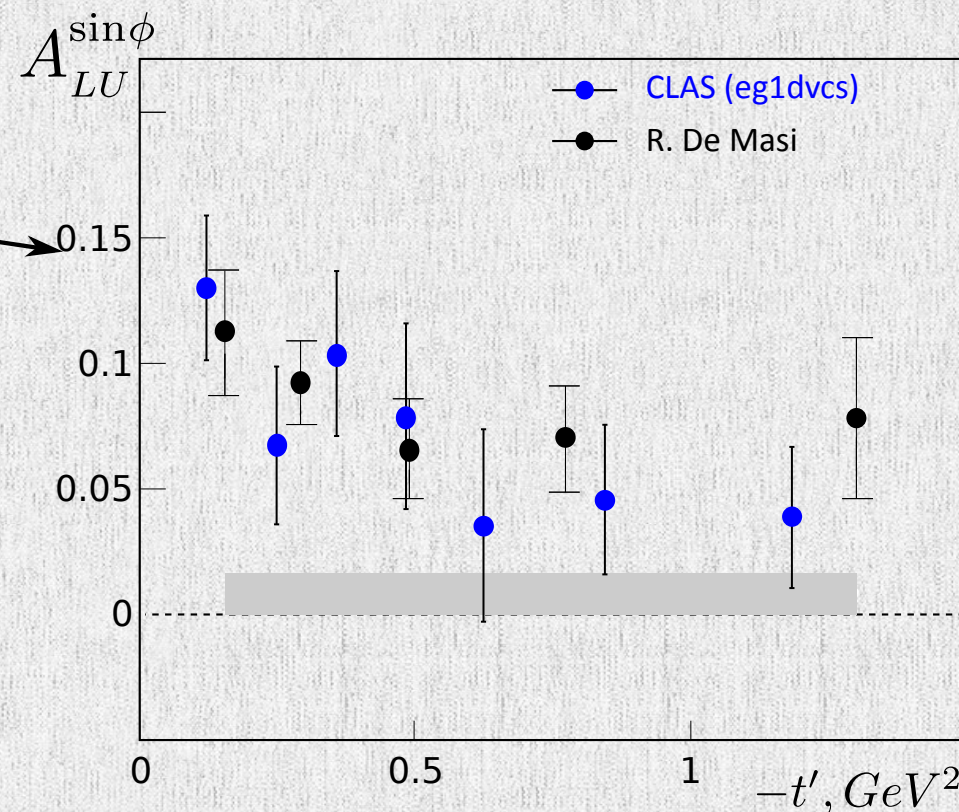
DV π^0 P BEAM SPIN ASYMMETRIES



R. De Masi et al. Measurement of $ep \rightarrow ep\pi^0$ beam spin asymmetries above the resonance region. *Phys.Rev.*, C77:042201, 2008.

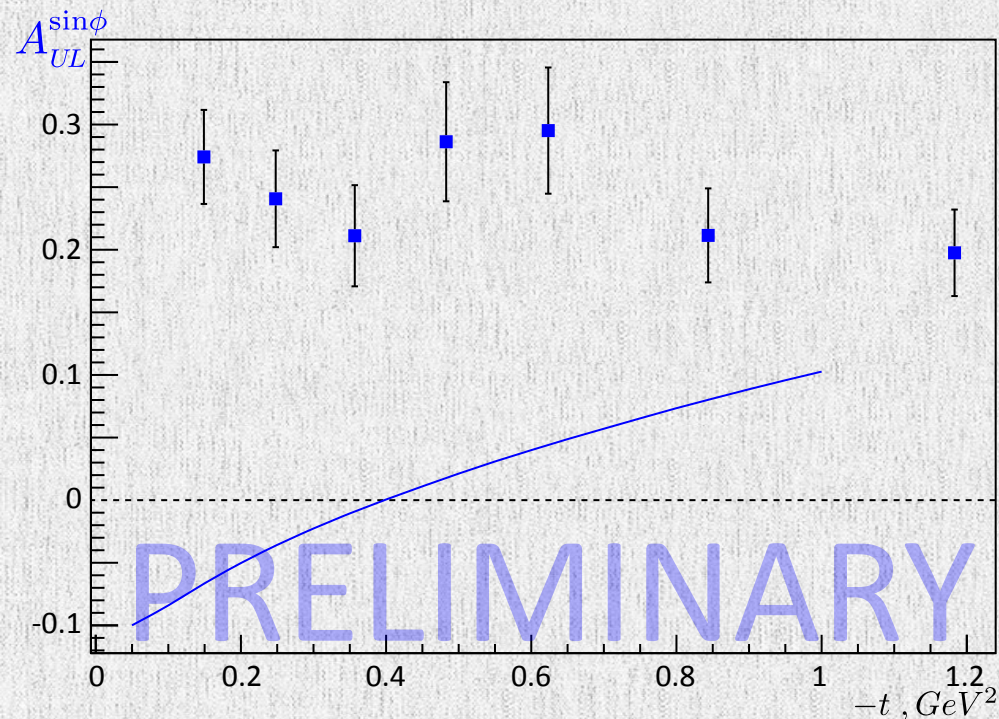
Red line is a Regge-type JML model.

- ◆ Good agreement with previous measurements on unpolarized target
- ◆ Non-zero beam spin asymmetries indicate that both transverse and longitudinal amplitudes participate in the process



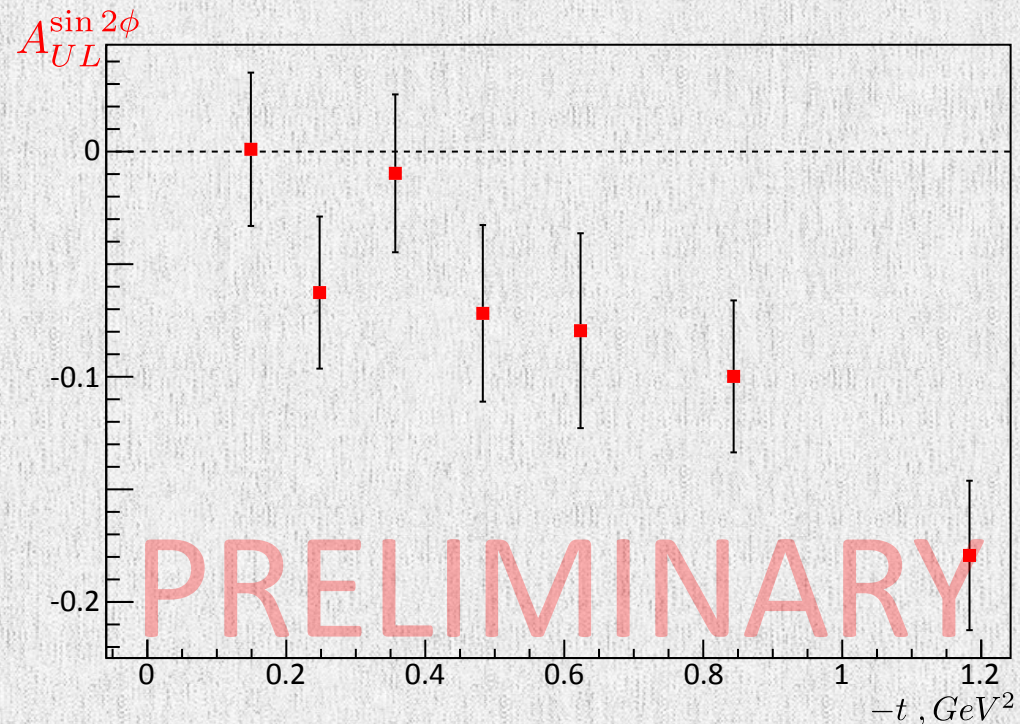
DV π^0 P TARGET SPIN ASYMMETRIES

$$A_{UL}^{\sin\phi} \sigma_0 \sim \text{Im} \left[\langle \bar{E}_T \rangle^* \langle \tilde{H} \rangle + \xi \langle H_T \rangle^* \langle \tilde{E} \rangle \right]$$



Detailed interpretations are model dependent and strongly influenced by new data. The understanding of discrepancy between them provides necessary information for further improvements.

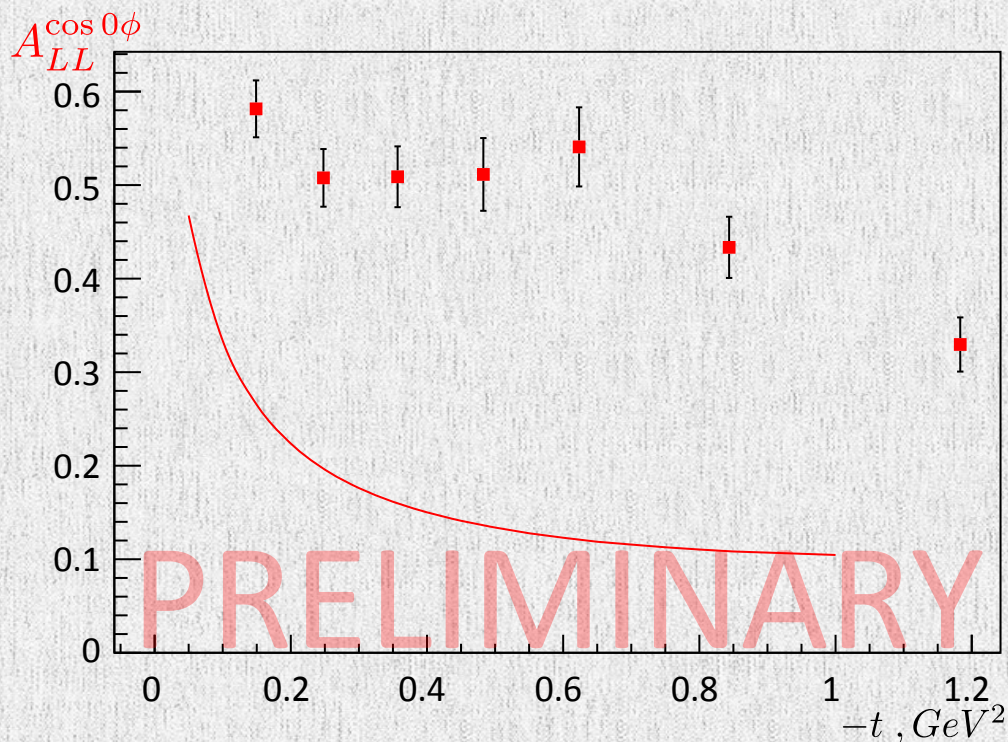
$$A_{UL}^{\sin 2\phi} \approx 0$$



Based on model calculation and assumptions this parameter is expected to be zero. It is consistent with experimental results in forward region, but deviates at higher t region.

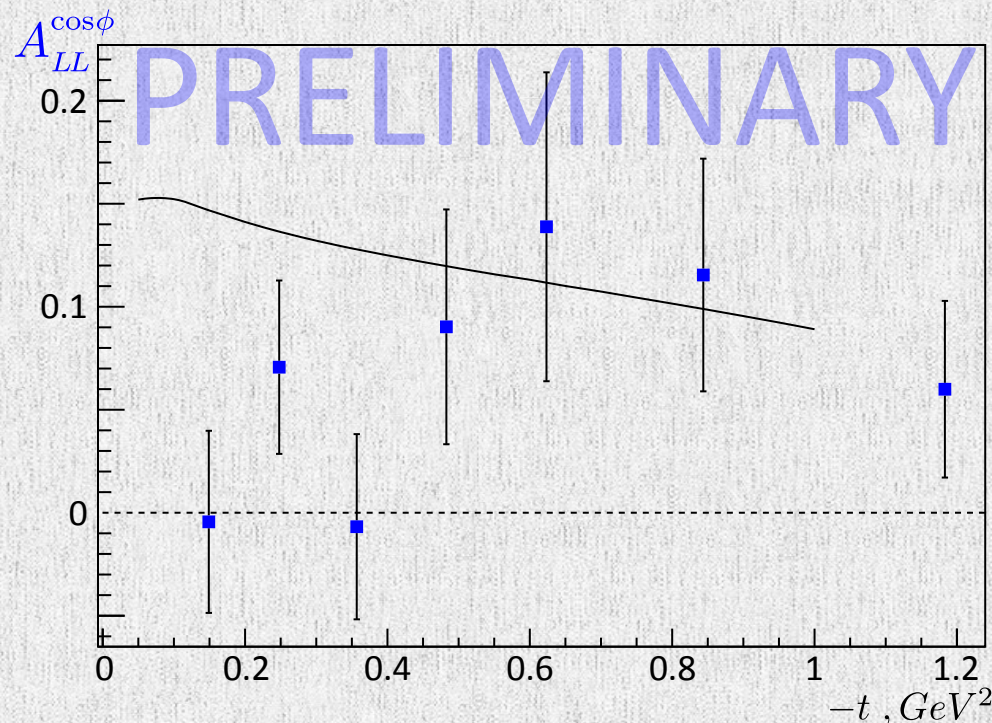
DV π^0 P DOUBLE SPIN ASYMMETRIES

$$A_{LL}^{\cos 0\phi} \sigma_0 \sim |\langle H_T \rangle|^2$$



The only experimental information on GPD H_T comes from HERMES measurements in π^+ electroproduction

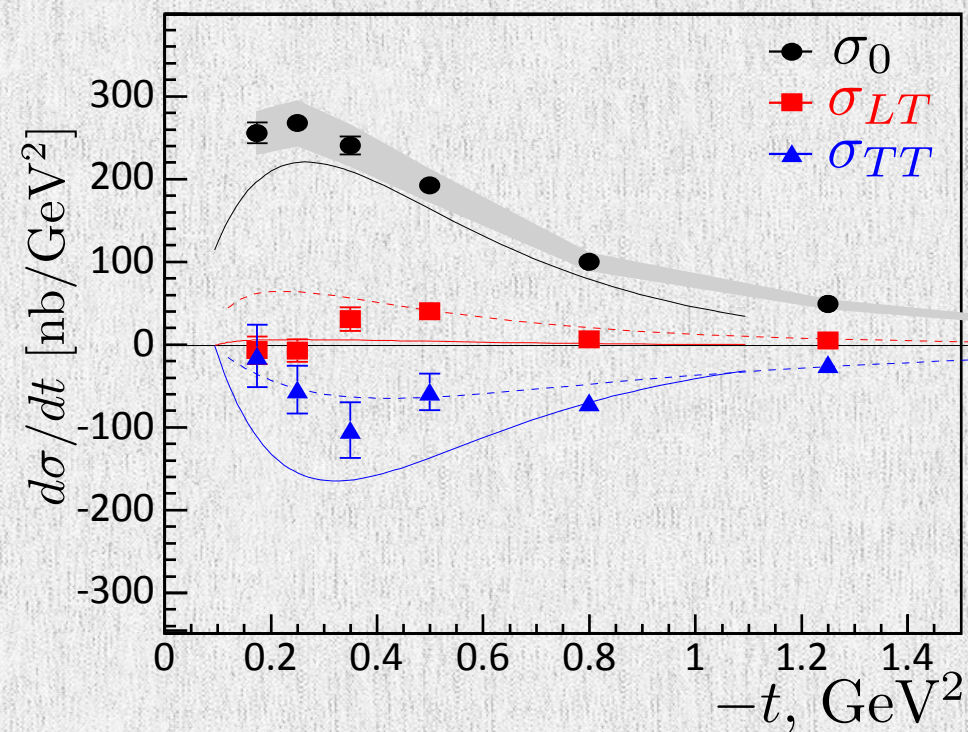
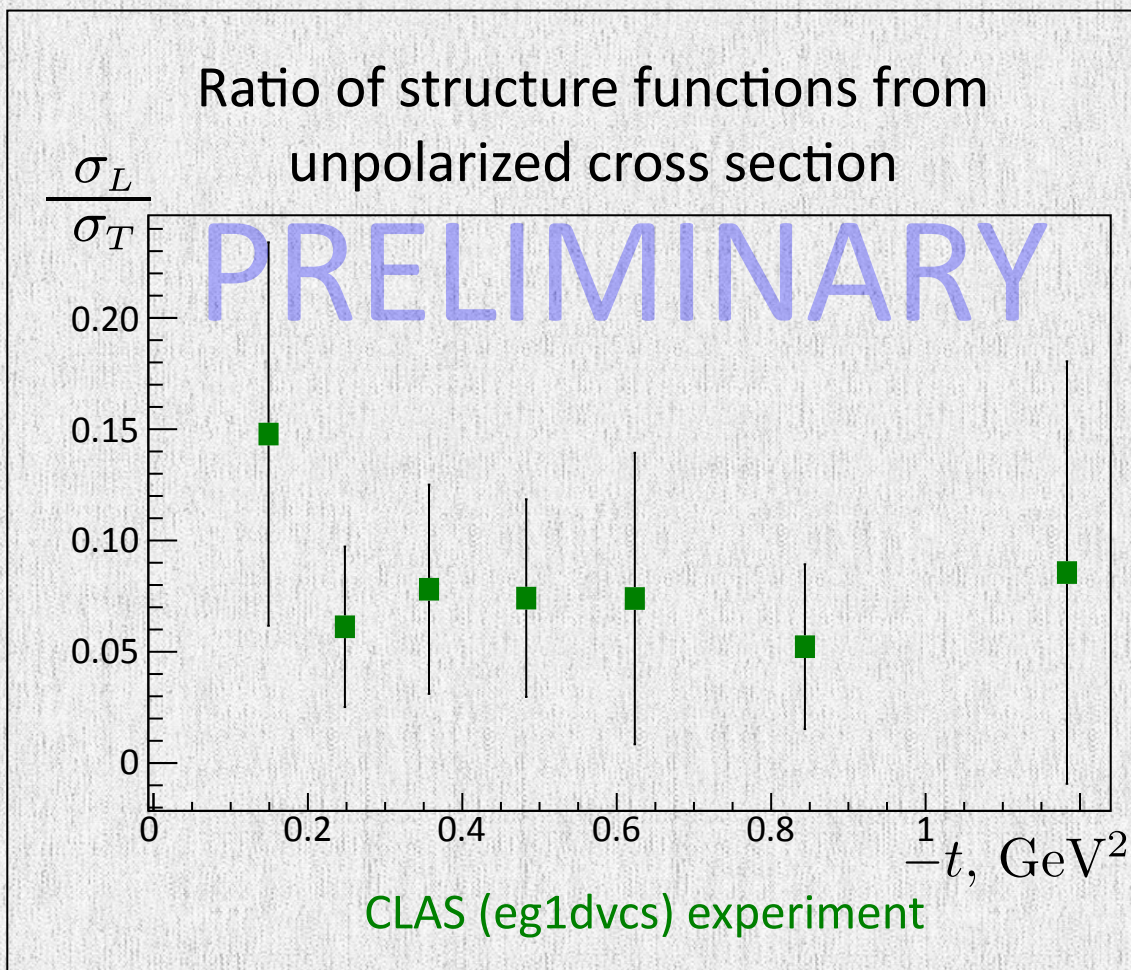
$$A_{LL}^{\cos \phi} \sigma_0 \sim \text{Re} \left[\langle \bar{E}_T \rangle^* \langle \tilde{H} \rangle + \xi \langle H_T \rangle^* \langle \tilde{E} \rangle \right]$$



$A_{UL}^{\sin \phi}$ and $A_{LL}^{\cos \phi}$ measure imaginary and real parts of the same combination of GPDs

TRANSVERSE PHOTON AMPLITUDES

- ◆ The theoretical approaches were developed utilizing chiral odd GPDs in the calculation of pseudoscalar electroproduction
- ◆ The data confirm the expectation that π^0 electroproduction is a uniquely sensitive process to access the transversity GPDs
- ◆ They lead to sizable transverse photon amplitudes, as *evidenced in the CLAS data*

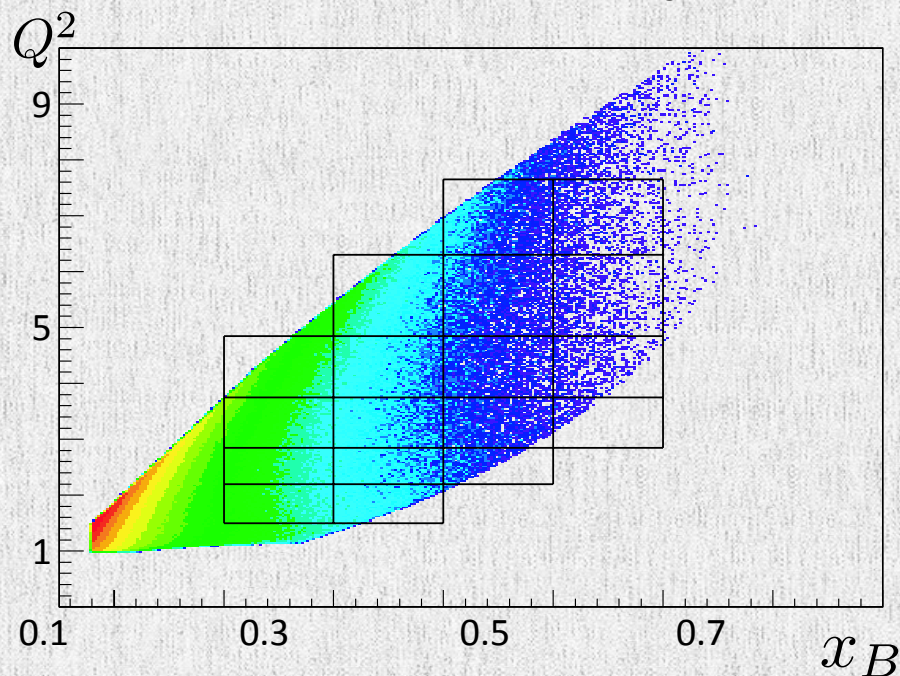


I. Bedlinskiy *et al.* Measurement of Exclusive π^0 Electroproduction Structure Functions and their Relationship to Transversity GPDs. 2012.

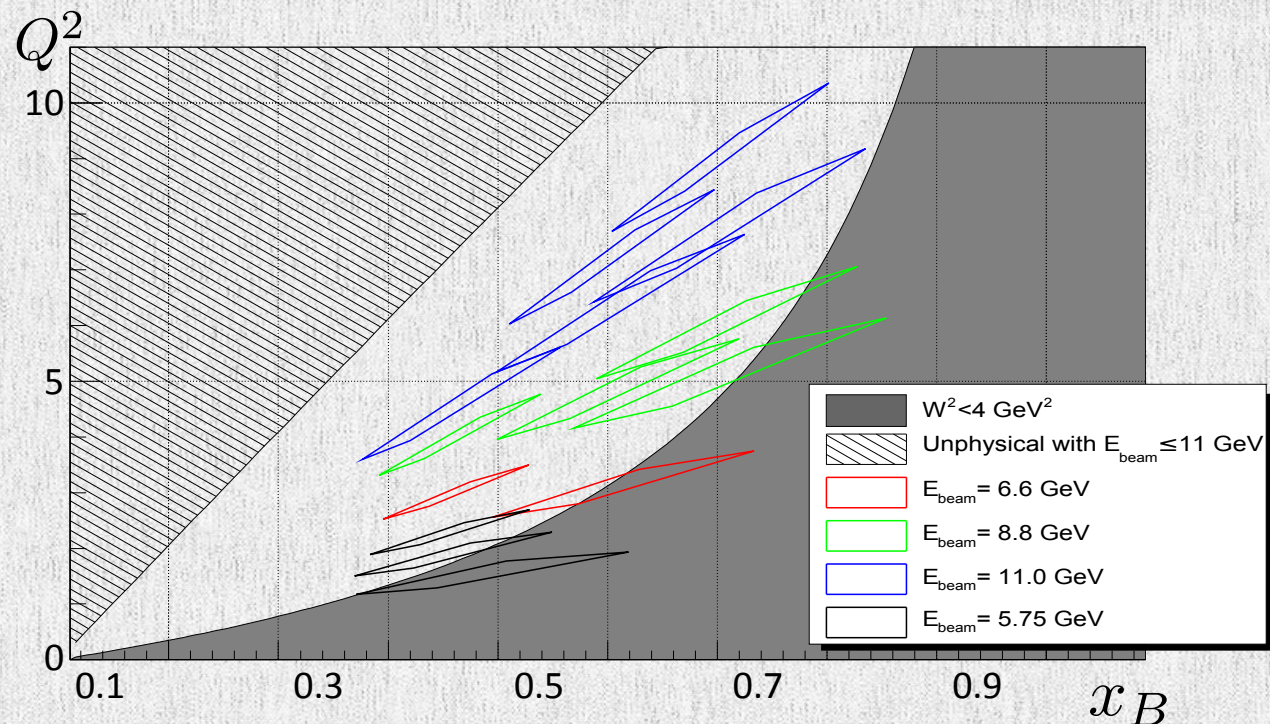
JLAB 12 GeV

The JLab 12 GeV project offers a large phase space acceptance for simultaneous detection of DVCS and DVMP channels.

CLAS12 kinematics for DVCS and DVMP on unpolarized H_2 and longitudinally polarized NH_3 target



Hall A kinematics for DVCS and DVMP electroproduction



Charles E. Hyde, Michel Guidal, and Anatoly V. Radyushkin. Deeply Virtual Exclusive Processes and Generalized Parton Distributions. *J.Phys.Conf.Ser.*, 299:012006, 2011.

SUMMARY

- ◆ Deeply exclusive photon and π^0 productions provide access to the full set of GPDs. The current (preliminary) data add new and sensitive information that will impact the extraction of GPDs from the data.
- ◆ The current DVCS data provide great sensitivity and kinematic coverage for the separation of H and \tilde{H} .
- ◆ For the first time, the preliminary target and double spin asymmetries for exclusive neutral pion electroproduction have been extracted from CLAS (eg1dvcs) data.
- ◆ Combination of polarized and unpolarized observables provide constraints for t dependence on underlying transverse GPDs and may well establish the role of transversity in pion electroproduction.
- ◆ The increased energy and luminosity after JLab 12 GeV upgrade will allow to extend the analysis at higher Q^2 and x_B and to perform Rosenbluth L/T separations.

Спасибо за приглашение!
Посещение Байкала было мечтой моей жизни.
Теперь эта мечта осуществилась.
Надеемся на дальнейшее плодотворное
сотрудничество.
Это большая честь для нас.

Thank you for invitation!
Visiting Baikal has been my dream for whole my life.
Now the Dream has come true.
We hope for further fruitful collaboration.
It is an honor for us.